中國機械工程學刊第四十二卷第三期第 295~301 頁(民國一百一十年)
Journal of the Chinese Society of Mechanical Engineers, Vol.42, No.3, pp 295~301 (2021)

Chassis Skin Temperature Transient Prediction Model of Electronics Devices

Sheng-Chao Lin *, Ruey Tsai *, Kuan-Yu Chen *and Chia-Pin Chiu **

Keyword: thermal transient prediction, chassis skin temperature, system performance, performance optimization

Abstract

An electronic device chassis skin temperature transient response prediction model is proposed. This model optimizes dynamic thermal control parameters using simulations. The thermal interaction between the chassis skin, chassis material and environment were analyzed and simplified into an energy balance equation. By solving this equation, chassis skin transient thermal response function corresponding to the processor temperature is established. The system prediction model was built after identifying the system parameters. This approach quickly establishes the chassis skin temperature transient model for an electronics system without complicated calculations or time consuming CFD modeling processing. The experimental data shows the error is within 1.43 °C (9.1%) and 6000 prediction calculation seconds within the Microsoft® Excel™ environment. This model benefits engineers interested in electronic device optimizing system performance using simulations.

Introduction

Modern electronic devices are stylish, slim and light weight. The highest device performance results in processor and chassis temperature thermal limit violation. Dynamic thermal control is the solution for balancing thermal constraints and system performance. The current method used to maximize system performance involves serial thermal tests that identify the optimized control policy parameters. This process is time and labor consuming.

Paper Received May, 2020. Revised November, 2020. Accepted December, 2020. Author for Correspondence: Sheng-Chao Lin

* *Department of Mechanical Engineering, Chung Yuan Christian University. No. 200, Chungpei Rd., Chungli District, Taoyuan City, Taiwan 32023, R.O.C.*

** *Intel Corporation, 5000 W. Chandler Blvd. Chandler, Az 85226, USA*

This process normally takes 2 to 3 days to complete. The process time is the area that can be improved for cost savings. The most efficient way to reduce the processing time is to replace the required thermal tests with thermal transient calculations. To achieve that goal, processor and chassis skin temperature thermal transient prediction models become necessary.

Several methods were proposed to build transient prediction models for topics variance. The finite difference method was used to determine the temperature rise in substation connectors (Abomailek et al. 2017) and multi-layer materials optimization to improve transient heat conduction (He et al. 2018). The Cauer network with finite discrete (Bagnoli et al. 1998, Magnone et al. 2013) or infinite continuous (Székely 1997, Székely et al. 2000) RC elements were used to build a dynamic thermal network to validate the thermal transient response discharge in silicon power devices for packaging failure analysis and inspection. Using finite element method to determine temperature-dependent structural parameters for the transient response prediction was discussed by Deng et al. (2016). The above methods require complicated mathematical calculations and a huge amount of computing time to determine system unknowns to build a transient prediction model. To improve the calculation efficiency, Merrikh (2015) proposed building a compacted thermal model in the finite volume method based on computational fluid dynamics (CFD) software to predict the transient hot spot temperature of a cell phone. Another approach acquires a transient solution solved from an energy balance equation to predict the thermal response. It was used on Loop Heat Pipes by Meinicke et al. (2019), solar receivers by Xu et al. (2018), multi-zone temperature control in a building by Woradechjumroen et al. (2016), workload and resource management simulations in computer systems by Piątek et al. (2015). Lin et al. (2019) proposed a lumped thermal capacity model to predict notebook PC transient processor temperature. Lin's model was developed for heat source thermal transient prediction. Based on the same concept, the proposed chassis skin temperature transient prediction model was built by extending the lumped system analysis range from the heat source point to a wider range from the heat source to chassis skin. The merit of this method is that it requires zero complicated model building and computing time with CFD software. It has fast calculations and is easy to use. The results show 6000 seconds of prediction calculation performed within one second in the Microsoft® Excel™ environment. The predicted results were checked for accuracy against the experimental measurement data. With limited error, we expect to benefit engineers interested in electronic device optimizing system performance using simulations.

Mathematical model

Figure 1 is an illustration of a heater cross section attached using a heat sink placed in an enclosure. Assuming P_{heater} of power generated from the heater flowing through a heat sink and enclosure chassis into ambient air produces heater temperature at T_{heater} and chassis skin temperature at T_{skin} when the ambient air temperature is T_a. The lumped thermal resistance between the heater and chassis skin is denoted as $R_1$and the lumped thermal resistance between chassis skin and ambient air is R_2. The specific chassis heat is $C_{p\_chassis}$ and the chassis mass at the hot spot is $m_{chassis}$. At any given instant, from the law of energy conservation, the energy generated from the heater equals the energy absorbed by the chassis material plus the energy flowing from the chassis into the ambient air, thus the energy balance from the heater into the ambient air can be described as equation (1).

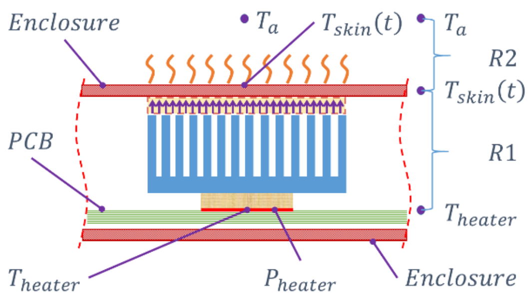

Figure 1. The illustration of the heater, heatsink and chassis skin temperature (hot spot) location

$$\frac{T_{heater}-T_{skin}(t)}{R_1} - m_{chassis} \cdot C_{p_{chassis}} \cdot \frac{dT_{skin}(t)}{dt} = \frac{T_{skin}(t)-T_a}{R_2}. \tag{1}$$

The chassis skin temperature $T_{skin}(t)$ in the first-order differential equation (1) can be solved as

$$T_{skin}(t) = \frac{T_a}{1+R'} + \left(T_{skin}(0) - \frac{T_a}{1+R'}\right) \cdot e^{-\frac{(1+R')}{\tau_{skin}} \cdot t} + \frac{T_{heater} \cdot R'}{1+R'} \cdot \left(1 - e^{-\frac{(1+R')}{\tau_{skin}} \cdot t}\right), \tag{2}$$

where τ_{skin} is called the time constant of the chassis, $\tau_{skin} = m_{chassis} \cdot C_{p\_chassis} \cdot R_2$, and R' is the ratio of R_1 and R_2, $R' = \frac{R_2}{R_1}$.

Two ways to determine R' and τ_{skin}. From the definition of R', it is the ratio of R_1 and R_2. R_1 is determined from heater and chassis skin temperature and heater power at steady state. R_2 is determined from chassis skin temperature and ambient air temperature and heater power at steady state. τ_{skin} is determined from the area of hot spot, thickness of the chassis, the property of the chassis material and R_2. The other way is to optimize R' and τ_{skin} through experimental data using mathematical technique such as Particle Swarm Optimization (PSO) (Lin et al. 2019).

The lumped system analysis model is applicable when the Biot number is less than 0.1. It is valid to analyze the power source question when the analysis range is close to a point. The lumped system analysis assumes that the internal conduction resistance is small compared with the surface convection resistance. Such analysis has the assumption of a uniform temperature throughout the system. The small conduction resistance indicates the system has a small diffusion time by neglecting the thermal diffusion effect. However, when extending the system to a range from the electronic device processor to chassis skin, the Biot number is obviously larger than 0.1. Thus, we will introduce a diffusion time into equation (2) to compensate for the large error in equation (4). The details are discussed in a later section.

Experimental arrangement

To assess the application of equation (2), two experiments were designed to evaluate the error by comparing the measurements and calculated temperature on the hot spot top side of an empty enclosure that contains a ceramic plate heater with step power applied in the first test to confirm the equation assumption. A server Thermal Test Vehicle (TTV) was used in a later test with step power applied to assess its application on a processor package heater. The application was evaluated on a HP® ProBook 640 G5 Notebook PC to evaluate its practical application. In the ceramic plate heater test setup, the heater was suspended inside a dummy box without any heat sink attached. In the server TTV test, a 260g Aluminum heat sink was attached to the TTV and a constant rotational speed blower provided constant air flow rate through this heat sink to dissipate heat. A 5 mm air gap was kept between the heat sink and enclosure. Figure 2 is an illustration of the server TTV test setup and the measured location of the skin, heater and ambient air temperature. Like the dummy box test, the Notebook PC skin temperature was measured on the top side chassis hot spot. During measurement step power was applied to a ceramic plate heater and server TTV to heat up the heater and TTV. A Notebook PC was applied with designed power pattern by executing Intel® Thermal Analysis Tool (TAT) to capture the processor and skin temperature. Generally, engineers evaluate a PC's calculation or graphical processing performance by executing a Central Processing Unit (CPU) or Graphics Processing Unit (GPU) intensive application such as Maxon® Cinebench R15 for CPU or UL Benchmarks® 3D Mark11 for GPU. While executing a CPU or GPU intensive application, heat concentrates in the processor calculative processing area or graphical processing area which causes uneven heat generation in the processor die because modern processors have integrated CPU and GPU on the same die. CPU and GPU intensive applications appear randomly in applications. Processor manufacturers such as Intel® define Thermal Design Power (TDP) for thermal engineers to design a PC's thermal solution based on a slightly balanced CPU and GPU intensive application. In the extreme application case, the CPU and GPU intensive application switches repeatedly, for example the switch workload between 100% CPU + 0% GPU workload and 0% CPU workload + 100% GPU workload repeatedly. The heat concentration on the processor die moves from the CPU area to the GPU area immediately and repeatedly. In the common application case, a light CPU workload application such as Microsoft® Office™ and GPU intensive application such as gaming applications switch repeatedly. To evaluate all conditions in the PC test, the TAT power pattern was designed to be TDP workload → CPU all 50% workload → GPU 100% workload → 3 minutes idle and repeated 5 times.

While measuring chassis skin temperature, both the dummy box test setup and Notebook PC were placed in LongWin LW-9022 HB nature convention chamber and the chamber temperature was set at 25°C. Table 1 is a summary of the applied power pattern or application to each test. Table 2 is a summary of the workload design for Notebook PC tests.

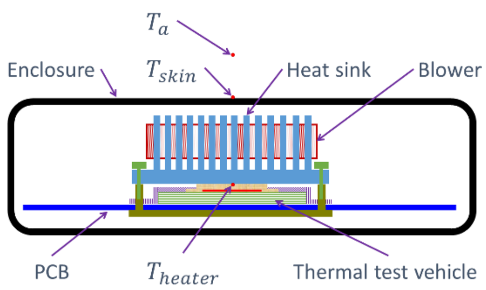

Figure 2. Illustration of the dummy box with server TTV test structure

Table 1. Matix of the experimental arrangement

Enclosure	Heater type	Power pattern / stress application
Dummy box	Ceramic plate heater	Step power
	Server TTV	Step power
Notebook PC	8th Generation Intel® Core™ i5 processor	TAT

Table 2. Workload design in the Notebook PC test

Application	Condition	Test loop
TAT	TDP workload → CPU all 50% workload → GPU 100% workload → 3 minutes idle	5

Results and discussion

Figures 3 and 4 show a comparison of the chassis skin temperature as a function of the time between the measured data and calculated data from equation (2). Figures 3a and 4a are the dummy box top side hot spot measure data vs. calculated chassis skin temperature. In the plots the amount of power supplied to the heater uses the right-hand-side y axis and the temperature uses the left-hand-side y axis. The Heater-Temp is the heater temperature, Tskin_top is the temperature measured on the top side chassis surface at hot spot, cal_Tskin is the calculated temperature from equation (2), and PWR-heater is the power applied to heater and PWR-TTV is the power applied to server TTV. Figures 3b and 4b are the error plots of the ceramic plate heater test and server TTV test. In dummy box tests, after a time 100 minutes for each experiment, the results showed that ceramic plate heater has 1.21°C error; Server TTV test has 2.24°C error. The error in those two tests occurred while the power has a violent variation.

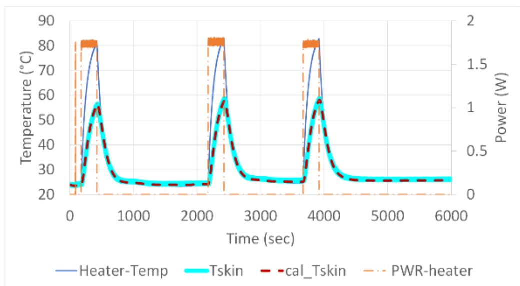

Figure 3a. Ceramic plate heater test result vs. calculated chassis skin temperature

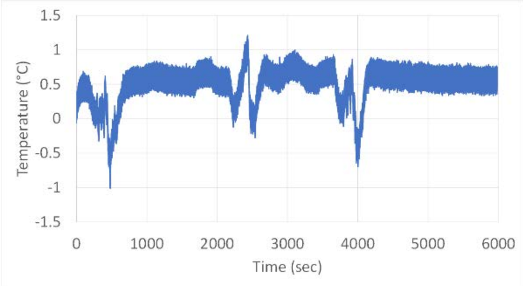

Figure 3b. The error plot of the ceramic plate heater test

Figure 3 The ceramic plate heater test result vs. calculated chassis skin temperature and error plots

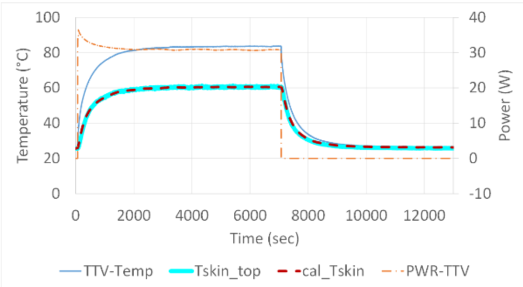

Figure 4a. The server TTV test result vs. calculated chassis skin temperature

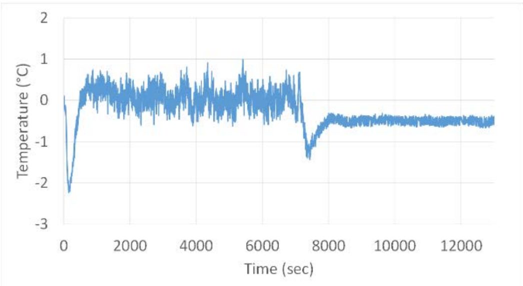

Figure 4b. The error plot of the server TTV test

Figure 4. The server TTV test result vs. calculated chassis skin temperature and error plots

Figure 5 is the Notebook PC TAT test result and calculated chassis skin temperature plot. In the plot the amount of processor power uses the right-hand-side y axis and temperature uses the left-hand-side y axis. The CPU-Temp is the processor temperature; the Tskin_top is the temperature measured on the top side chassis surface at the hot spot. cal_Tskin is the calculated temperature from equation (2), and PWR-CPU is the processor power consumption. In the TAT test the error is 1.34°C. As with the dummy box test the error occurred while the processor power has a violent variation. To evaluate equation (2) in the industrial measurement system performance condition, two more Notebook PC tests were performed while executing Cinebench R15 and 3D Mark11. The results show the Cinebench R15 test has 2.46°C error and 3D Mark11 test has 1.58°C error. All test results indicate that equation (2) well predicts the chassis skin temperature along with the time and the error is within 2.46 °C in all test conditions.

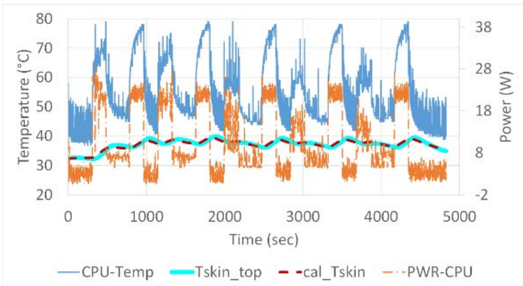

Figure 5. Notebook TAT test result vs. calculated chassis skin temperature

The R' and τ_{skin} values used for equation (2) in all cases above were optimized by PSO and the corresponding error are tabulated in Table 3.

Table 3 The optimized R' and τ_{skin} by PSO and the error in each test

	Heater type / Application	R'	τ_{skin} (sec)	Error (°C)
Dummy box test	Ceramic plate heater	1.532	123.23	1.21
	Server TTV	1.466	177.55	2.24
Notebook PC test	TAT	0.523	587.10	1.34
	Cinebench	0.425	592.13	2.46
	3DMark 11	0.462	584.22	1.58

Define

$$\text{percentage of error} = \frac{Error}{T_{rise}} = \frac{T_{skin} - T_{prediction}}{T_{skin,peak} - T_a}, \quad (3)$$

where T_{skin} is the temperature measured from the chassis skin top side hot spot. $T_{prediction}$ is the temperature calculated from equation (2). T_{rise} is the temperature difference between the peak hot spot temperature and ambient temperature. $T_{skin,peak}$ is the measured peak hot spot temperature on the chassis skin top side. T_a is the ambient air temperature.

From the test data, the heater mass and structure impact equation (2) accuracy. From the dummy box test results, a heavier and more complicated heater structure is less accurate than a lighter and simpler heater structure. For example, the server TTV test (2.24 °C, 8.8% error) prediction has larger error than the ceramic plate heater test (1.21 °C, 4.9% error). The error occurred when power was suddenly applied to the heater or TTV. In the Notebook PC test results, larger error occurred while applications were launched from idle or power inducing violent variations. The data indicate that it is because of the time delay in the chassis skin temperature response when compared with the prediction due to heat diffusion. Equation (2) assumes that the total amount of heat generated from the heater flows immediately through the chassis into the ambient air, however, the power propagation is slower than the assumption due to diffusivity. The time delay is a function of the material diffusivity between the heat source and chassis skin and higher diffusivity shortens the delay. Compared with 260g of Al heat sink attached to server TTV and TTV structure, the ceramic plate heater has a simpler material combination and smaller mass, which leads to a shorter time delay with better accuracy. Not taking diffusion time into the calculation results in faster temperature response in the prediction. This is easier to observe, especially when the system is under dynamic power pattern stress. To compensate for the delay behavior, equation (2) is rewritten as:

$$T_{skin}(t) = \frac{T_a}{1+R\prime} + \left(T_{skin}(t_0) - \frac{T_a}{1+R'}\right) \cdot e^{-\frac{(1+R')}{\tau_{skin}} \cdot t} + \frac{T_{heater}(t-t_{diffussion}) \cdot R\prime}{1+R\prime} \cdot \left(1 - e^{-\frac{(1+R')}{\tau_{skin}} \cdot t}\right), \quad (4)$$

where $t_{diffusion}$ is defined as the time when power propagates from heat source to chassis and starts to effect chassis skin temperature.

$t_{diffusion}$ can be determined from system test data by using Least Square Method. From Notebook PC test, $t_{diffusion}$ was identified as 60 seconds in all three application tests. Introducing $t_{diffusion}$ improves the accuracy from 15.61% to 9.1% in Cinebench test. The improvement by using equation (4) is tabulated in Table 4. Figure 6 is the error plot of the Cinebench tests with and without $t_{diffusion}$. In this case, $t_{diffusion}$ improves accuracy throughout the entire test range.

Table 4. Error comparison: Results with and without 60 second of $t_{diffusion}$

Notebook PC test	$t_{diffusion}$ = 0 sec		$t_{diffusion}$ = 60 sec	
	°C	%	°C	%
TAT	1.34	11.32	1.06	8.97
Cinebench	2.46	15.61	1.43	9.1
3DMark 11	1.58	10.90	1.11	7.67

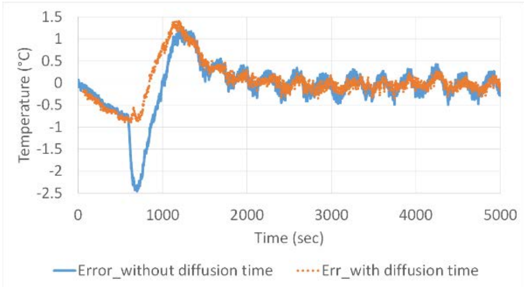

Figure 6 Error comparison: Cinebench test result with and without 60 seconds of $t_{diffusion}$

From the PC test results, even on the same Notebook PC, the R' value varies with the executing applications. TAT has slightly balanced CPU and GPU power distribution with the largest R' value (0.523), Cinebench R15 has CPU intensive power distribution with the smallest R' value (0.462) and the R' value (0.425) of the GPU intensive power distribution application, 3D Mark11, is in the middle. The interaction between applications or power distribution on the processor die with R' value has not yet been investigated. It might be because of application processing power consumption, system fan rotational speed control mechanism, the CPU and GPU ratio processing area on the processor die or a combination of the above items. Further study is needed to characterize applications or power distribution on the processor die to R' value.

Conclusion

The goal of the presented work is to develop a method to predict electronic device transient chassis skin temperature for optimizing dynamic thermal control policy parameters using simulations. The experimental data indicates the proposed model, equation (2), provides less than 2.46°C (15.61%) error and the majority are within 1°C if without $t_{diffusion}$ compensation. Introducing $t_{diffusion}$ for compensation improves the error to 1.43 °C (9.1%) and reduces error throughout entire test. τ_{skin} and R' can be identified from the test data using PSO if the system has been built or estimated from CFD software tool calculations if the system is in the design stage. This method is fast in transient calculations with adequate accuracy but avoids the model building process and lengthy computational time.

References

Ali Akbar Merrikh, "Compact thermal modeling methodology for predicting skin temperature of passively cooled devices", Applied Thermal Engineering, Vols. 85 PP. 287-296 (2015)

C. Abomailek, F. Capelli, J.-R. Riba, P. Casals-Torrens, "Transient thermal modelling of substation connectors by means of dimensionality reduction", Applied Thermal Engineering, 111 (2017) 562–572

Denchai Woradechjumroen, Yuebin Yu, Haorong Li, "Virtual partition surface temperature sensor based on linear parametric model", Applied Energy, 162 (2016) 1323–1335

Ke-Lun He, Qun Chen, En-fu Dong, Wei-Chun Ge, Jun-Hong Hao, Fei Xu, "An improved unit circuit model for transient heat conduction performance analysis and optimization in multi-layer materials", Applied Thermal Engineering, 129 (2018) 1551–1562

Li Xu, Wesley Stein, Jin-Soo Kim, Zhifeng Wang, "Three-dimensional transient numerical model for the thermal performance of the solar receiver", Renewable Energy, 120 (2018) 550-566

P. E. Bagnoli, C. Casarosa, M. Ciampi, and E. Dallago, "Thermal resistance analysis by induced transient (TRAIT) method for power electronic devices. Thermal characterization —Part I: Fundamental and theory", IEEE Transactions on Power Electronics, 13 (6) (1998) 1208-1219

P. Magnone, C. Fiegna, G. Greco, G. Bazzano, S. Rinaudo, E. Sangiorgi, "Numerical simulation and modeling of thermal transient in silicon power devices", Solid-State Electronics, 88 (2013) 69–72

S. C. Lin, R. Tsai, C. P. Chiu, L. k. Liu, "A Simple Approach for System Level Thermal Transient Prediction", Thermal Science and Engineering Progress, Vols. 9, PP. 177-184 (2019).

S. C. Lin, R. Tsai, K. Y. Chen, C. C. Chien, "Application of Particle Swarm Optimization Algorithm in Power Source Thermal Transient Prediction", ICECC 2019: Proceedings of the 2019 2nd International Conference on Electronics, Communications and Control Engineering, Pages 7–11, April (2019).

Sebastian Meinicke, Paul Knipper, Christoph Helfenritter, Thomas Wetzel, "A lean approach of modeling the transient thermal characteristics of Loop Heat Pipes based on experimental investigations", Applied Thermal Engineering, 147 (2019) 895–907

V. Székely, "A new evaluation method of thermal transient measurement results", Microelectronics Journal, 28 (3) (1997) 277–292

V.Székely, A. Poppel, M. Rencz, "Algorithmic Extension of Thermal Field Solvers: Time Constant Analysis", Sixteenth Annual IEEE Semiconductor Thermal Measurement and Management Symposium, San Jose, CA, USA, Mar. 23, 2000

Wojciech Piątek, Ariel Oleksiak, Georges Da Costa, "Energy and thermal models for simulation of workload and resource management in computing systems", Simulation Modelling Practice and Theory, 58 (2015) 40–54

Z. Deng, Z. Guo, X. Zhang, "Non-probabilistic set-theoretic models for transient heat conduction of thermal protection systems with uncertain parameters", Applied Thermal Engineering, 95 (2016) 10–17

Abbreviation

CFD	Computational Fluid Dynamics
CPU	Central processing unit
GPU	Graphics processing unit
ILM	Independent loading mechanism
PC	Personal computer
TAT	Intel® Thermal Analysis Tool
TTB	Thermal test board
TTV	Thermal test vehicle

Nomenclature

$C_{p\_chassis}$	the specific heat of the chassis	$J/kg \cdot K$
$m_{chassis}$	represented chassis mass	Kg
P_{heater}	heater power	W
R'	the ratio between R_1 and R_2, $R' = \frac{R_2}{R_1}$	-
R_1	the lumped thermal resistance from heater to chassis	$°C/W$
R_2	the lumped thermal resistance from chassis to ambient air	$°C/W$
T_a	ambient air temperature	$°C$
T_{heater}	Heater temperature	$°C$
T_{skin}	chassis skin temperature	$°C$
$T_{skin,peak}$	measured peak chassis temperature	$°C$
$t_{diffussion}$	the time when power propagates from heat source	sec

	to chassis skin and starts to effect chassis temperature	
T_{heater}	heater temperature	$°C$
$T_{prediction}$	temperature calculated from equation (2)	$°C$
T_{rise}	temperature difference	$°C$
τ_{skin}	time constant of the chassis	Sec

電子產品機殼表面溫度之暫態預測模型

林昇照 蔡瑞益 陳冠宇
私立中原大學機械工程學系

邱嘉斌
美商英特爾股份有限公司

摘要

探討欲利用數值模擬以最佳化動態熱管理控制機制之參數，而發展之電子產品機殼表面溫度暫態預測模型．此法透過能量平衡方程式，求得機殼表面溫度之暫態函數，經由代入系統參數後而建立．省卻複雜計算程序，及耗時之計算流體力學軟體工具建模過程．預測誤差在攝氏 1.43 度或 9.1%之內，且 6000 秒的暫態計算可在一秒內完成．期望對系統效能最佳化有興趣之工程師們有所助益．